***Available online at*** www.pelagiaresearchlibrary.com

**Pelagia Research Library**

**Advances in Applied Science Research, 2014, 5(5):249-259**

**ISSN: 0976-8610**
**CODEN (USA): AASRFC**

# Steady slip blood flow through a stenosed porous artery

**Manish Gaur and Manoj Kumar Gupta**

*Department of Mathematics, Government College, Kota, Rajasthan, India*

**ABSTRACT**

*Laminar steady flow taking blood as Casson fluid through a cylindrical artery with porous walls has been studied under slip stenotic conditions. The porous slip boundary conditions are taken as suggested by the Beavers and Joseph (1967). The results for the various flow characteristics like axial velocity, plug flow velocity, flow flux, wall shear stress and the pressure gradient have been discussed analytically and graphically under suitable flow parameters.*

**Keywords**: Casson Fluid; Stenosis; Slip Boundary Condition; Yield Stress; Porosity.

## INTRODUCTION

It is believed that the abnormal and the unnatural deposits of the fatty and the fibrous tissues in arterial lumen obstruct the blood flow which gives rise to various cardiovascular and cerebral diseases. According to medical reports, the endothelial walls have the ultra – microscopic pores for filtration. Cholesterol increases the wall permeability when the arterial walls are damaged, inflamed or dilated. When the fatty and fibrous tissues are clotted in the wall lumen, its distribution acts like a porous medium. Many researchers have attempted to understand the different flow features by considering blood flow through a porous cylindrical tube under stenosis.

G.S. Beavers et al. [1] studied the boundary conditions at a naturally permeable wall and suggested that the effect of boundary should be replaced with a slip velocity proportional to the exterior velocity gradient. D.F. Young [2] investigated the effect of time dependent stenosis on blood flow through a tube taking blood as a Newtonian fluid. R.K. Dash et al. [3] investigated the Casson fluid flow in a pipe filled with a homogeneous porous medium by applying the Brinkman model for the Darcy resistance shown by the porous medium. B.K. Mishra et al. [4] studied the effect of porous parameter and stenosis height on the wall shear stress of human blood flow. S. Mishra et al. [5] discussed the effects of the wall permeability through a stenosed artery. D. Jogie et al. [6] studied the laminar flows of two immiscible fluids through permeable channel. A. Kumar et al. [7] investigated the porous effects on two phase blood under magnetic field. S. Pramanik [8] used Casson fluid model to study the boundary layer fluid flow with heat transfer past an exponentially porous stretching surface under the thermal radiation and observed that the skin-friction increases when the suction parameter increases. Gaur and Gupta [9] discussed a Casson fluid model for steady flow through a stenosed blood vessel in which authors explained that the axial velocity, volumetric flow rate and pressure gradient increase with the increase in slip velocity and decrease with growth in yield stress. Gaur and Gupta [10] studied the slip effects on steady flow through a stenosed blood artery and found that axial velocity, volumetric flow rate and pressure gradient decrease along the radial distance as the slip length increases but the wall shear stress increases with increase in slip length. Gaur and Gupta [11] also analyzed the magnetic effects on steady blood flow through an artery under axisymmetric stenosis and concluded that the axial velocity and flow flux increase as the magnetic field gradient and slip velocity increase but they decrease with the stenosis height along axial distance.

## 2 MATHEMATICAL FORMULATION

Steady, laminar and incompressible flow of blood through an axially symmetric stenosed cylindrical artery in z – direction is considered.

The geometry of the stenosed artery is given below:

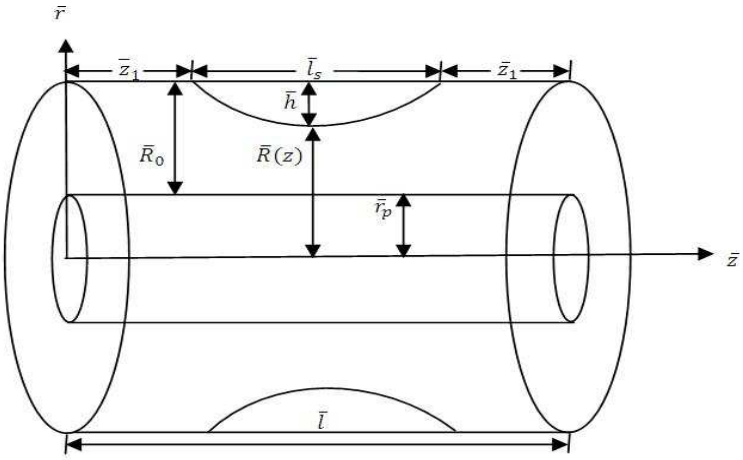


Let $\bar{R}_0$ be the radius of the normal tube and $\bar{R}(\bar{z})$ be the radius of the stenosed portion given by [2] as:

$$\bar{R}(\bar{z}) = \begin{cases} \bar{R}_0 - \frac{\bar{h}}{2}\left[1 + \cos\frac{2\pi}{\bar{l}_s}(\bar{z}_1 + \bar{l}_s - \bar{z})\right]; & \bar{z}_1 \le \bar{z} \le \bar{z}_1 + \bar{l}_s \\ \bar{R}_0 & ;\ \text{otherwise} \end{cases} \tag{2.1}$$

Where $\bar{l}_s$ is the length of the stenosis in the artery of the length $\bar{l}$, $\bar{z}_1$ is the position of the stenosis of maximum height $\bar{h}$. Let $\bar{r}$ and $\bar{z}$ be radial and axial coordinates respectively.

The blood is considered to behave like Casson fluid passing through the artery having permeable walls of homogeneous and isotropic materials. Flow is considered to be governed by the Darcy's Law.

With above considerations, the equations of motion in the dimensional form are:

$$-\frac{\partial \bar{p}}{\partial \bar{z}} + \frac{1}{\bar{r}}\frac{\partial}{\partial \bar{r}}(\bar{r}\bar{\tau}_c) = 0 \tag{2.2}$$

$$\frac{\partial \bar{p}}{\partial \bar{r}} = 0 \tag{2.3}$$

Where $\bar{p}$ is the pressure at any point and $\bar{\tau}_c$ be the shear stress of the Casson fluid with following simplified constitutive equations:

$$F(\bar{\tau}_c) = -\frac{\partial \bar{v}_c}{\partial \bar{r}} = \frac{1}{\bar{k}_c}\left(\bar{\tau}_c^{1/2} - \bar{\tau}_0^{1/2}\right)^2 \quad \text{for } \bar{\tau}_c \ge \bar{\tau}_0 \tag{2.4}$$

$$\frac{\partial \bar{v}_c}{\partial \bar{r}} = 0 \qquad \text{for } \bar{\tau}_c \le \bar{\tau}_0 \tag{2.5}$$

where $\bar{v}_c$ is the axial velocity of the blood, $\bar{\tau}_0$ be the yield stress and $\bar{k}_c$ is the fluid viscosity.

The equations (2.2) to (2.5) are subject to the following boundary conditions [1]:

$$\left.\begin{aligned} &\bar{\tau}_c = \text{Finite Value} && \text{at } \bar{r} = 0 \\ &\bar{v}_c = \bar{v}_s && \text{at } \bar{r} = \bar{R}(\bar{z}) \\ &\frac{\partial \bar{v}_c}{\partial \bar{r}} = \frac{\alpha}{\bar{\epsilon}^{1/2}}(\bar{v}_s - \bar{v}_f) && \text{at } \bar{r} = \bar{R}(\bar{z}) \end{aligned}\right\} \tag{2.6}$$

Where by Darcy's law,

$$\bar{v}_f = -\frac{\bar{\epsilon}}{\bar{k}_c}\frac{\partial \bar{p}}{\partial \bar{z}} \tag{2.7}$$

Here $\bar{v}_s$ represents the slip velocity in $z$ – direction, $\bar{v}_f$ is the filter velocity of fluid through the porous region known as the Darcy value, $\alpha$ be a non – dimensional quantity known as the slip parameter which depends upon the material parameters characterizing the structure of porous material within the boundary region and $\bar{\epsilon}$ is the permeability of the wall material.

Introducing the following non – dimensional variables as

$$R(z) = \frac{\bar{R}(\bar{z})}{\bar{R}_0},\ z = \frac{\bar{z}_1 + \bar{l}_s - \bar{z}}{\bar{l}_s},\ r = \frac{\bar{r}}{\bar{R}_0},\ \tau_c = \frac{\bar{\tau}_c}{\bar{p}_0\bar{R}_0/2},\ \tau_0 = \frac{\bar{\tau}_0}{\bar{p}_0\bar{R}_0/2},\ v_c = \frac{\bar{v}_c}{\bar{p}_0\bar{R}_0^2/2\bar{k}_c},\ v_s = \frac{\bar{v}_s}{\bar{p}_0\bar{R}_0^2/2\bar{k}_c},$$
$$v_f = \frac{\bar{v}_f}{\bar{p}_0\bar{R}_0^2/2\bar{k}_c},\ H = \frac{\bar{h}}{\bar{R}_0},\ \epsilon = \frac{\bar{\epsilon}}{\bar{R}_0^2},\ \frac{\partial p}{\partial z} = \frac{\partial \bar{p}/\partial \bar{z}}{\bar{p}_0} \tag{2.8}$$

Here $\bar{p}_0$ denotes the steady – state amplitude.

With above non – dimensional scheme, the radius of the stenotic area of the artery becomes

$$R(z) = \begin{cases} 1 - H\cos^2 \pi z\,; & 0 \le z \le 1 \\ 1 & ;\ \text{otherwise} \end{cases} \tag{2.9}$$

Non – dimensional forms of equations (2.2) to (2.5) are

$$-2\frac{\partial p}{\partial z} + \frac{1}{r}\frac{\partial}{\partial r}(r\tau_c) = 0 \tag{2.10}$$

$$\frac{\partial p}{\partial r} = 0 \tag{2.11}$$

$$-\frac{\partial v_c}{\partial r} = (\tau_c^{1/2} - \tau_0^{1/2})^2 \qquad \text{for } \tau_c \ge \tau_0 \tag{2.12}$$

$$\frac{\partial v_c}{\partial r} = 0 \qquad \text{for } \tau_c \le \tau_0 \tag{2.13}$$

The dimensionless slip boundary conditions are

$$\left.\begin{aligned} &\tau_c = \text{Finite Value} && \text{at } r = 0 \\ &v_c = v_s && \text{at } r = R(z) \\ &\frac{\partial v_c}{\partial r} = \frac{\alpha}{\epsilon^{1/2}}(v_s - v_f) && \text{at } r = R(z) \end{aligned}\right\} \tag{2.14}$$

$$\text{where } v_f = -2\epsilon\frac{\partial p}{\partial z} \tag{2.15}$$

Applying condition (2.14) in equation (2.10), the shear stress $\tau_c$ and wall shear stress $\tau_R$ are obtained as:

$$\tau_c = -r\frac{\partial p}{\partial z} \tag{2.16}$$

$$\tau_R = -R\frac{\partial p}{\partial z} \tag{2.17}$$

From equations (2.16) and (2.17),

$$\frac{\tau_c}{\tau_R} = \frac{r}{R} \tag{2.18}$$

where $R = R(z)$

## METHOD OF SOLUTION

Integrating equation (2.12) under conditions (2.14) and using the result (2.15), the velocity in the region $r_p \le r \le R(z)$ where $r_p = \frac{\bar{r}_p}{\bar{R}_0}$ being the non – dimensional radius of the plug flow region, is given as:

$$v_c = \frac{R}{2\tau_R}\left[(\tau_R^2 - \tau_c^2) - \frac{8}{3}\tau_0^{1/2}\left(\tau_R^{3/2} - \tau_c^{3/2}\right) + 2\tau_0(\tau_R - \tau_c)\right] - \frac{\in^{1/2}}{\alpha}\left(\tau_R^{1/2} - \tau_0^{1/2}\right)^2 + \frac{2\in\tau_R}{R} \tag{3.1}$$

Within plug flow region i.e. $0 \le r \le r_p$, $\tau_c = \tau_0$ at $r = r_p$, therefore the plug flow velocity is

$$v_p = \frac{R}{2\tau_R}\left[\tau_R^2 - \frac{1}{3}\tau_0^2 - \frac{8}{3}\tau_0^{1/2}\tau_R^{3/2} + 2\tau_0\tau_R\right] - \frac{\in^{1/2}}{\alpha}\left(\tau_R^{1/2} - \tau_0^{1/2}\right)^2 + \frac{2\in\tau_R}{R} \tag{3.2}$$

Now the volumetric flow rate in the dimensionless form for the region $0 \le r \le R(z)$ is obtained as:

$$Q = 4\int_0^R r v(r) dr`$$

$$= 4\int_0^{r_p} r v_p dr + 4\int_{r_p}^R r v_c dr$$

Hence

$$Q = \frac{R^3}{2\tau_R^3}\left(\tau_R^4 - \frac{16}{7}\tau_0^{1/2}\tau_R^{7/2} + \frac{4}{3}\tau_0\tau_R^3 - \frac{1}{21}\tau_0^4\right) - \frac{2\in^{1/2}}{\alpha}R^2\left(\tau_R^{1/2} - \tau_0^{1/2}\right)^2 + 4\in R\tau_R \tag{3.3}$$

If $\tau_0 \ll \tau_R$ i.e. $\frac{\tau_0}{\tau_R} \ll 1$, then equation (3.3) becomes

$$Q = \frac{R^3}{2}\left(\tau_R - \frac{16}{7}\tau_0^{1/2}\tau_R^{1/2} + \frac{4}{3}\tau_0\right) - \frac{2\in^{1/2}}{\alpha}R^2\left(\tau_R^{1/2} - \tau_0^{1/2}\right)^2 + 4\in R\tau_R \tag{3.4}$$

which gives us the wall shear stress for the stenosed artery as

$$\tau_R = \left[\frac{\varphi_1}{2\varphi_3}\tau_0^{1/2} + \left\{\frac{42\alpha Q}{\varphi_3} + \frac{(\varphi_1^2 - 4\varphi_2\varphi_3)}{4\varphi_3^2}\tau_0\right\}^{1/2}\right]^2 \tag{3.5}$$

Where

$$\left.\begin{aligned} \varphi_1 &= 24R^2\left(2\alpha R - 7\in^{1/2}\right) \\ \varphi_2 &= 28R^2\left(\alpha R - 3\in^{1/2}\right) \\ \varphi_3 &= 21R\left(\alpha R^2 - 4R\in^{1/2} + 8\alpha\in\right) \end{aligned}\right\} \tag{3.6}$$

The pressure gradient is obtained by using equation (3.5) in equation (2.17) as:

$$\frac{\partial p}{\partial z} = -\frac{1}{R}\left[\frac{\varphi_1}{2\varphi_3}\tau_0^{1/2} + \left\{\frac{42\alpha Q}{\varphi_3} + \frac{(\varphi_1^2 - 4\varphi_2\varphi_3)}{4\varphi_3^2}\tau_0\right\}^{1/2}\right]^2 \tag{3.7}$$

## RESULTS AND DISCUSSION

The velocity profile for the axial velocity in the non – plug flow region has been derived in equation (3.1) and the graphical discussions of the results are mentioned in figures 1(a) and 1(b).

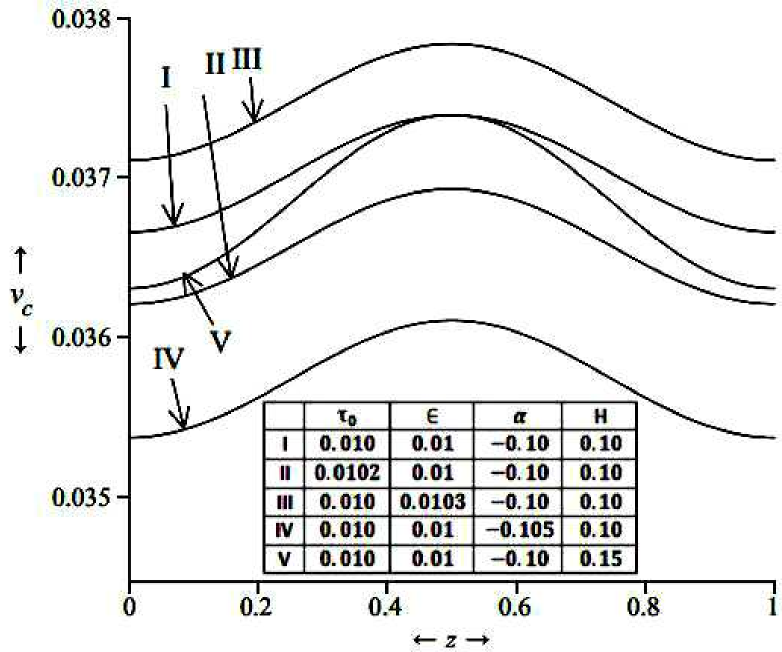


Figure 1 (a): Variation of Axial velocity Along Axial Distance for Different Values of the Permeability ∈, Slip Parameter $\alpha$, Stenosis Height $H$ and Yeild Stress $\tau_0$ with Some Fixed Values $\tau_R = 0.070$ and $\tau_c = 0.030$

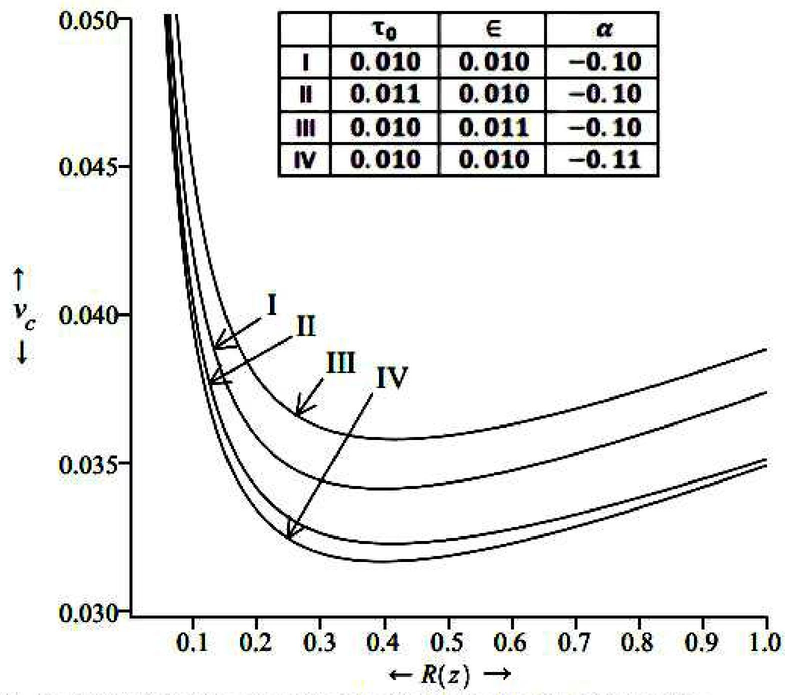


Figure 1 (b): Variation of Axial velocity Along Radial Distance for Different Values of the Permeability ∈, Slip Parameter $\alpha$, and Yeild Stress $\tau_0$ with Some Fixed Values $\tau_R = 0.070$ and $\tau_c = 0.030$.

Figure 1(a) shows the changes in the axial velocity along axial distance for the different values of the permeability $\in$, slip parameter $\alpha$, stenosis height H and yield stress $\tau_0$ with some fixed values $\tau_R = 0.070$ and $\tau_c = 0.030$. The axial velocity increases when the wall permeability increases but it decreases when slip parameter, stenosis height and the yield stress increase.

Figure 1(b) represents the variations of the axial velocity versus radial distance for the various values of the permeability $\in$, slip parameter $\alpha$ and yield stress $\tau_0$ with some fixed values $\tau_R = 0.070$ and $\tau_c = 0.030$. The graph of axial velocity shows a fall up to the stenosis and then rise along the radius of the artery. The axial velocity increases with increase in wall permeability whereas it decreases as slip parameter and yield stress increase.

The graphical details of the axial velocity for the plug flow area obtained through equation (3.2) has been shown in figures 2(a) and 2(b).

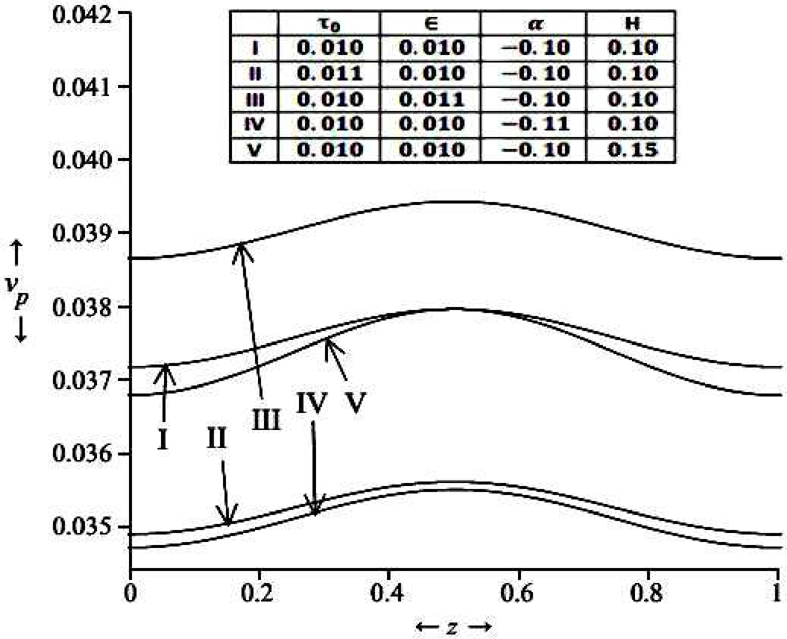


**Figure 2 (a): Variation of Plug Flow Velocity Along Axial Distance for Different Values of the Permeability $\in$, Slip Parameter $\alpha$, Stenosis Height $H$ and Yeild Stress $\tau_0$ with Some Fixed Values $\tau_R = 0.070$ and $\tau_c = 0.030$.**

Figure 2(a) gives the variations in plug flow velocity along the arterial axis for different values of the permeability $\in$, stenosis height H and yield stress $\tau_0$ with some fixed values $\tau_R = 0.070$ and $\tau_c = 0.030$. The plug flow velocity increases with increase in the wall permeability but it decreases when the yield stress, slip parameter and the stenosis height increase.

Figure 2(b) shows the variations in plug flow velocity along radial distance for the various values of the permeability $\in$ and yield stress $\tau_0$ with some fixed values $\tau_R = 0.070$ and $\tau_c = 0.030$. The general behaviour of plug flow velocity is to decrease initially and then to increase with increments in radial distance. The plug flow velocity increases with the permeability but it decreases with the yield stress and slip parameter.

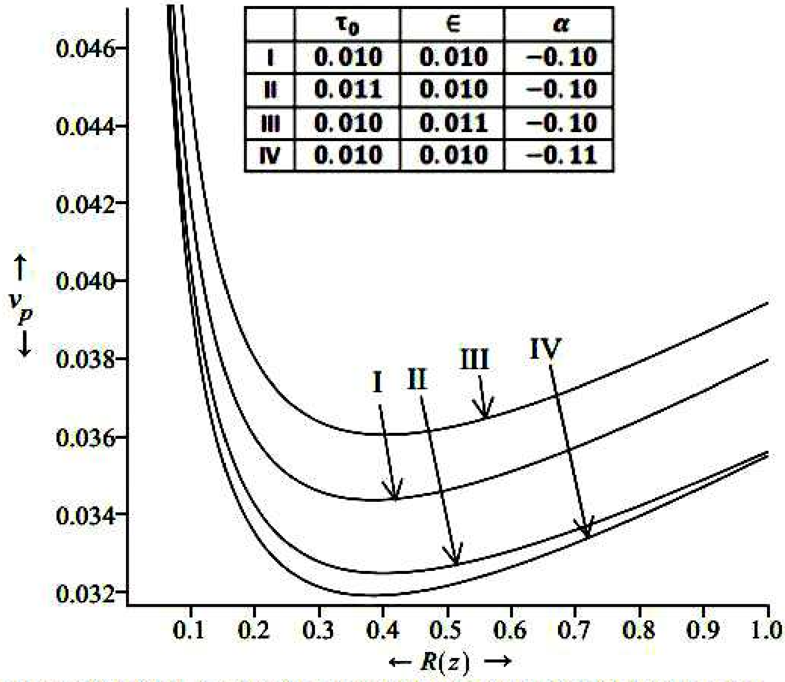


Figure 2 (b): Variation of Plug Flow Velocity Along Radial Distance for Different Values of the Permeability $\in$, Slip Parameter $\alpha$ and Yeild Stress $\tau_0$ with Some Fixed Values $\tau_R = 0.070$ and $\tau_c = 0.030$.

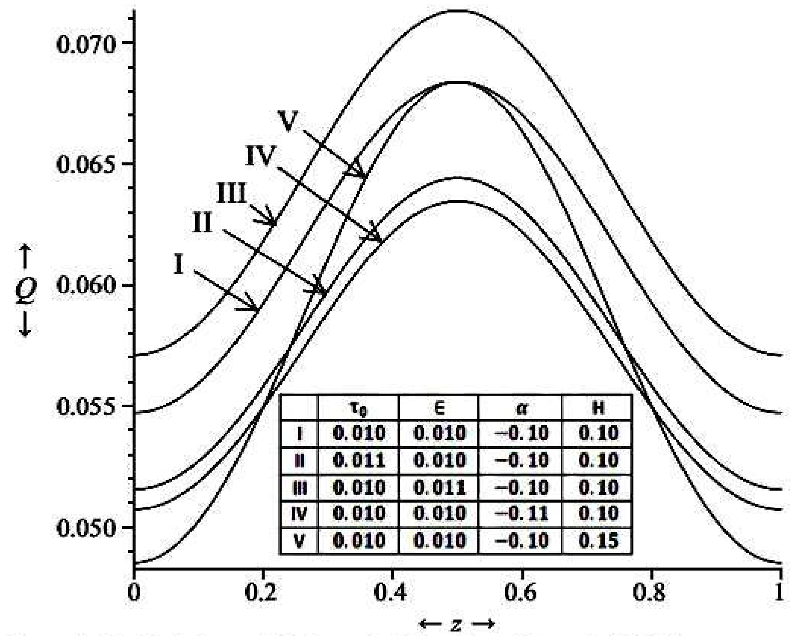


Figure 3 (a): Variation of Volumetric Flow Rate Along Axial Distance for Different Values of the Permeability $\in$, Slip Parameter $\alpha$, Stenosis Height $H$ and Yeild Stress $\tau_0$ with Some Fixed Values $\tau_R = 0.070$ and $\tau_c = 0.030$.

The variations of the volumetric flow rate obtained through equation (3.4) are plotted against the axial distance for the various values of the permeability $\in$, slip parameter $\alpha$, stenosis height H and yield stress $\tau_0$ with some fixed values $\tau_R = 0.070$ and $\tau_c = 0.030$ in figure 3(a). The figure shows that flow flux increases when the wall permeability increases but it decreases as the slip parameter, stenosis height and the yield stress increase.

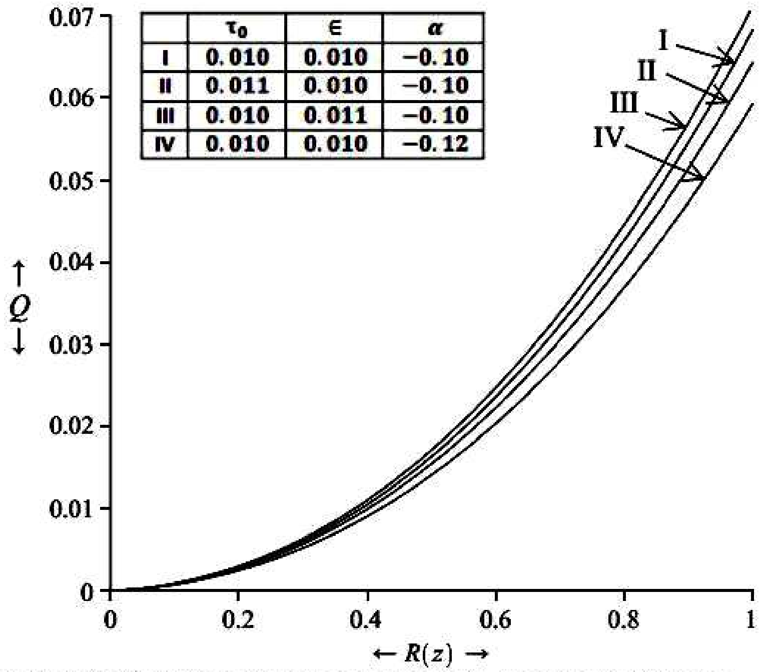


**Figure 3 (b): Variation of Volumetric Flow Rate Along Radial Distance for Different Values of the Permeability $\in$, Slip Parameter $\alpha$, and Yeild Stress $\tau_0$ with Some Fixed Values $\tau_R = 0.070$ and $\tau_c = 0.030$.**

Figure 3(b) shows the variation in the volumetric flow rate versus the radial distance for the different values of the permeability $\in$, slip parameter $\alpha$ and yield stress $\tau_0$ with some fixed values $\tau_R = 0.070$ and $\tau_c = 0.030$. The flow flux increases with increase in radial distance and the permeability and decreases with the increase in wall slip parameter and the yield stress.

Figure 4(a) represents the variations of the wall shear stress obtained through equation (3.5) along axial distance for different values of the permeability $\in$, slip parameter $\alpha$, stenosis height H and yield stress $\tau_0$ with some fixed values $\tau_R = 0.070$, $\tau_c = 0.030$ and $Q = 1$. The wall shear stress increases with increase in the stenosis height, yield stress and the wall slip but it decreases as the wall permeability increases.

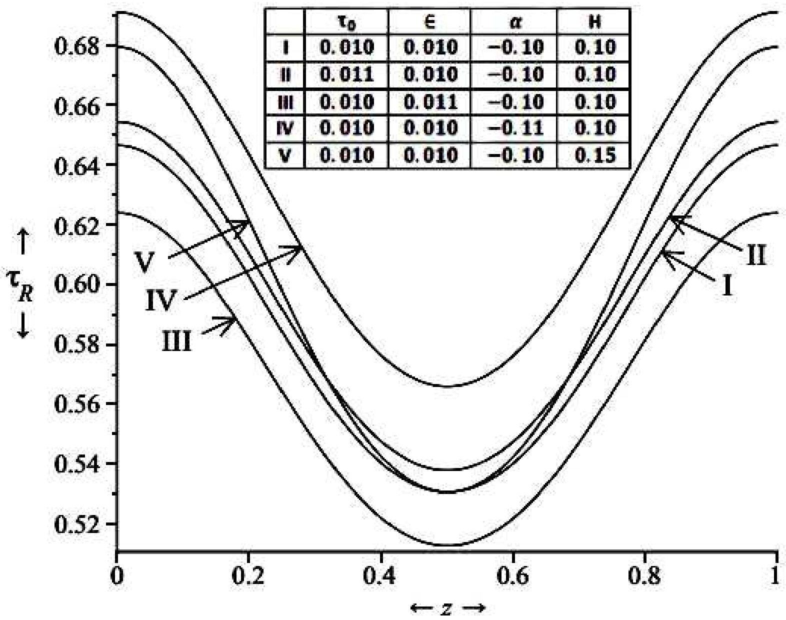


Figure 4 (a): Variation of Wall Shear Stress Along Axial Distance for Different Values of the Permeability $\in$, Slip Parameter $\alpha$, Stenosis Height $H$ and Yeild Stress $\tau_0$ with Some Fixed Values $\tau_R = 0.070$, $\tau_c = 0.030$ and $Q = 1$

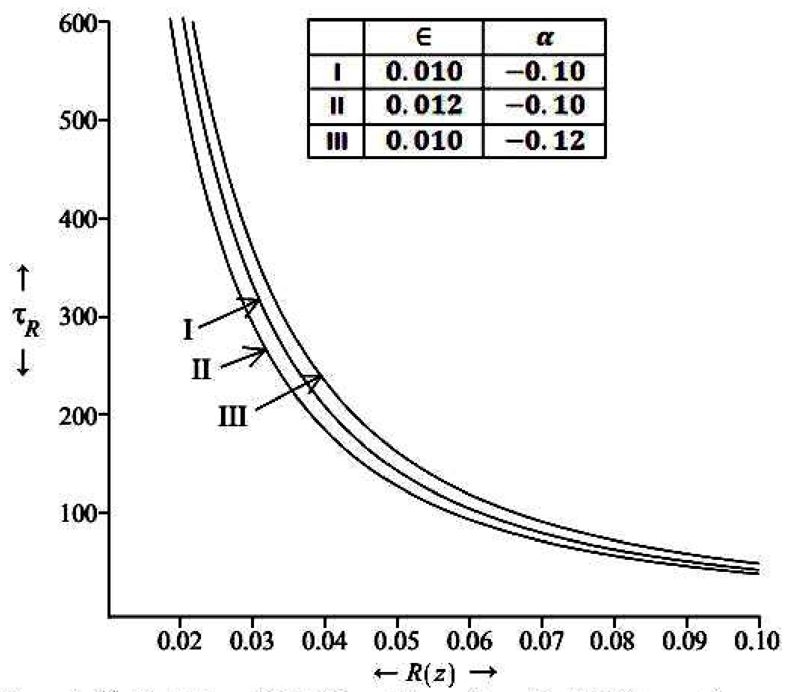


Figure 4 (b): Variation of Wall Shear Stress Along Radial Distance for Different Values of the Permeability $\in$ and Slip Parameter $\alpha$ with Some Fixed Values $\tau_R = 0.070$, $\tau_c = 0.030$, $\tau_0 = 0.010$ and $Q = 1$.

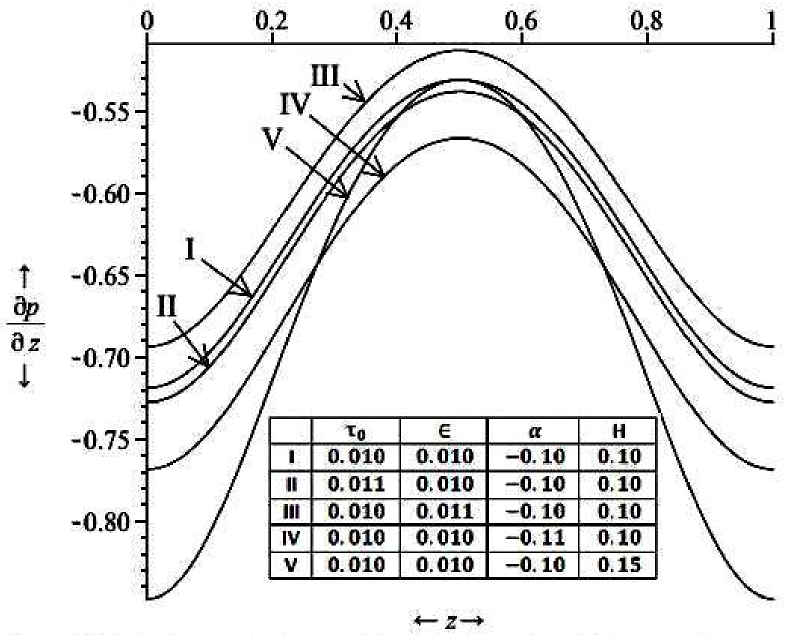


Figure 5 (a): Variation of Pressure Gradient Along Axial Distance for Different Values of the Permeability $\in$, Slip Parameter $\alpha$, Stenosis Height $H$ and Yeild Stress $\tau_0$ with Some Fixed Values $\tau_R = 0.070$, $\tau_c = 0.030$ and $Q = 1$.

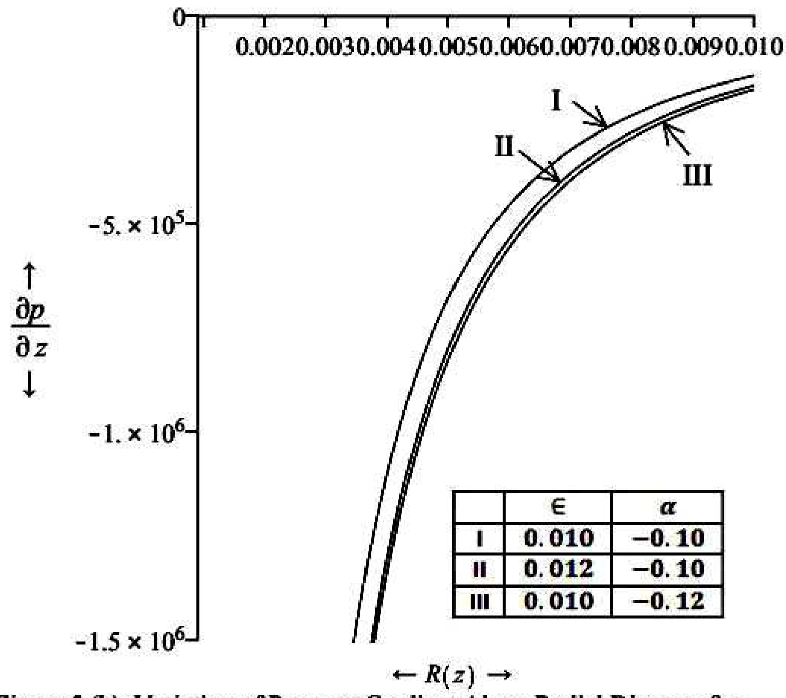


Figure 5 (b): Variation of Pressure Gradient Along Radial Distance for Different Values of the Permeability $\in$ and Slip Parameter $\alpha$ with Some Fixed Values $\tau_R = 0.070$, $\tau_c = 0.030$, $\tau_0 = 0.010$ and $Q = 1$.

Figure 4(b) shows the variation of wall shear stress along the radial distance for the different values of the permeability $\in$ and slip parameter $\alpha$ with some fixed values $\tau_R = 0.070$, $\tau_c = 0.030$ and $Q = 1$. The wall shear stress decreases as the wall permeability increases while it increases when the wall slip increases.

Figure 5(a) shows the variations of the pressure gradient derived through equation (3.7) along the axial distance for the different values of the permeability $\in$, slip parameter $\alpha$, stenosis height H and yield stress $\tau_0$ with some fixed values $\tau_R = 0.070$, $\tau_c = 0.030$ and $Q = 1$. The figure shows that pressure gradient increases with increase in the wall permeability while it decreases as the slip parameter, yield stress and the stenosis height increase.

Figure 5(b) represents variations of the pressure gradient versus the radial distance for the different values of the permeability $\in$, slip parameter $\alpha$, stenosis height H and yield stress $\tau_0$ with some fixed values $\tau_R = 0.070$, $\tau_c = 0.030$ and $Q = 1$. The pressure gradient exhibits increase along the arterial axis. It decreases with the increase in the permeability and the wall slip.

Table 1 shows the variations of the wall shear stress and the pressure gradient versus yield stress along the radial distance. It exhibits that the wall shear stress decreases with increase in radial distance but it increases as the yield stress increases. The pressure gradient increases with the increase in radial distance and decreases when the yield stress increases.

**Table 1: Wall Shear Stress and Pressure Gradient versus Radial Distance and Yield Stress.**

| $\tau_0$ | R = 0.1 | | R = 0.5 | | R = 1.0 | |
|---|---|---|---|---|---|---|
| | $\tau_R$ | $\frac{\partial p}{\partial z}$ | $\tau_R$ | $\frac{\partial p}{\partial z}$ | $\tau_R$ | $\frac{\partial p}{\partial z}$ |
| 0.010 | 41.8948388 | - 418.9483880 | 1.98300960 | - 3.9458527 | 0.5307037 | - 0.9770396 |
| 0.015 | 42.1387770 | - 421.3877703 | 2.04537614 | - 4.0600265 | 0.5642221 | - 1.0223947 |
| 0.020 | 42.3448658 | - 423.4486586 | 2.09866980 | - 4.1558355 | 0.5932526 | - 1.0614074 |

## CONCLUSION

The study shows that the axial velocity in both plug and non – plug flow regions, flow flux and the pressure gradient increase along axial and radial distances when the arterial wall becomes more porous. The wall shear stress decreases with increase in the wall porosity but it decreases as the slip parameter along axial and radial distances. Also the skin friction decreases when the stenosis height increases along axial distance. The axial velocity, flow flux and the pressure gradient decrease along the axial distance when the slip parameter and the stenosis height increase. The axial velocity, plug flow velocity, flow flux decrease along axial distance when yield stress increases which verifies the author's previous work [9].

## REFERENCES

[1] Beavers GS and Joseph DD, *J. Fluid Mech.*, **1967**, 30 (1): 197 – 207.
[2] Young DF, *J. Engg. For Ind., Trans of ASME*, **1968**, 90: 248 – 254.
[3] Dash RK, Mehta KN and Jayaraman G, *Int. J. Eng. Sc.*, **1996**, 34, No. 10: 1145 – 1156.
[4] Mishra BK and Verma N, *Res. J. Medicine and Medical Sc.*, **2007**, 2: 98 – 101.
[5] Mishra S, Siddiqui SU and Medhavi A, *Applications and Applied Math.*, **2011**, Vol. 6, Issue 11: 1798 – 1813.
[6] Jogie D and Bhatt B, *Int. J. Pure and Appl. Math.*, **2012**, Vol. 78, No. 3: 435 – 449.
[7] Kumar A, Varshney CL and Singh VP, *Appl. Math.*, **2012**, 2 (5): 166 – 170.
[8] Pramanik S, *Ain Shams Eng. J.*, **2014**, 5: 205 – 214.
[9] Gaur M and Gupta MK, *BJMC*, **2014**, Vol. 4(11): 1629 – 1641.
[10] Gaur M and Gupta MK, *IJSER*, **2014**, Vol. 5, Issue 2: 753 – 758.
[11] Gaur M and Gupta MK, *IJIAS*, **2014**, Vol. 8, No. 1: 394 – 407.